2009 IEEE International Conference on Robotics and Automation
Kobe International Conference Center
Kobe, Japan, May 12-17, 2009

Humanoid Robot *LOLA*

Sebastian Lohmeier, Thomas Buschmann, Heinz Ulbrich
Institute of Applied Mechanics, Technical University Munich 85748 Garching, Germany
{lohmeier,buschmann,ulbrich}@amm.mw.tum.de

***Abstract*—This paper presents our new 25-DoF humanoid walking robot *LOLA*. The goal of our research is to realize a fast, human-like walking motion (target speed: 5 km/h). Furthermore, we want to increase the robot's autonomous, vision-guided walking capabilities. The robot has 25 degrees of freedom, including 7-DoF legs with actively driven toe joints. It is characterized by its lightweight construction, a modular, multi-sensory joint design with brushless motors and an electronics architecture using decentralized joint controllers. Special emphasis was put on an improved mass distribution of the leg apparatus to achieve good dynamic performance. The sensor system comprises absolute angular sensors in all links, two custom-made force/torque sensors in the feet and a high-precision inertial sensor in the upper body. Trajectory generation and control system aim at faster, more flexible, and more robust walking patterns.**

I. Introduction

Recent developments in enabling technologies (biped walking control, mechatronics, computer technology) have lead to the design of sophisticated humanoid robots. Prominent examples are *ASIMO* [1], *H7* [2], *HRP-2* [3] and *HRP-3* [4], the *TOYOTA PARTNER ROBOT* [5], *WABIAN-2* [6] and *HUBO* [7]. With the biped robot *JOHNNIE* which was developed at our institute from 1998 to 2003, a maximum walking speed of 2.4 km/h has been achieved [8].

Possible future uses of such robots are in service, entertainment and academics, all of which require stable and fast biped locomotion as a basic skill. Even though research has been extended to more complex tasks in recent years — compared with human beings— higher walking speeds still remain challenging for most robots.

Obviously, the control problems inherent in fast walking are a very challenging field, since there are still many unsolved problems, e. g. fast walking and running [9], [10], sudden turning motions, walking on rough terrain and trajectory generation in complex environments. In our opinion, however, a careful design of the mechatronic system is essential, and should not be underestimated. Rather, all components must be seen as tightly coupled parts of a highly integrated mechatronic system.

In this paper we give an overview of the system, the mechatronic design concept, the mechanical design, the sensor system and the electronics architecture.

II. System Overview

Fig. 1 shows our new humanoid walking robot *LOLA*. The robot is 180 cm tall and weighs approximately 55 kg. Its physical dimensions are based on anthropometric data.

LOLA's hardware approach is based on experiments with *JOHNNIE* and tries to settle most of the technical problems discovered during a thorough hardware analysis. The distinguishing characteristics of *LOLA* are the redundant kinematic structure with 7-DoF legs, an extremely lightweight construction and a modular joint design using brushless motors. The mass distribution of the leg apparatus is improved to achieve good dynamic performance. The sensor system was revised in order to improve signal quality and bandwidth. Table I summarizes the key data of the robot.

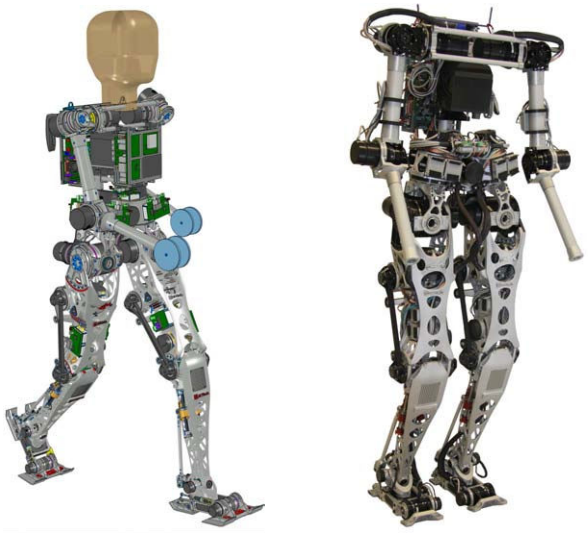

Figure 1. CAD drawing and photograph of the 25-DoF humanoid walking robot *LOLA*

Table I
Hardware Specification

General	Height	180 cm
	Weight	approx. 55 kg
	Total DoFs	25
	Maximum Walking Speed (Target)	5 km/h
	Power supply	external
Legs	7 DoFs (3 hip, 1 knee, 2 ankle, 1 toe)	
	Thigh length	440 mm
	Shank length	430 mm
	Foot height	105 mm
	Distance between hip joints	246 mm

A. Kinematic Structure

Simulations and experiments have shown that additional DoFs in a redundant configuration allow to implement more natural and flexible gait patterns and to extend the abilities of the robot in general. Fig. 2 shows the kinematic configuration with 25 actively driven DoFs: The legs have 7 DoFs each, the

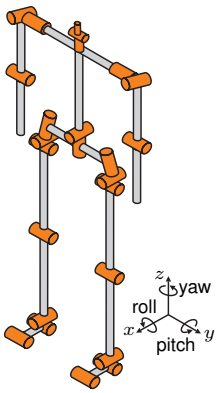

Joint	DoF
Head	3*
Shoulder	2
Elbow	1
Pelvis	2
Hip	3
Knee	1
Ankle	2
Toe	1
Total	**25**

* under development

Figure 2. Kinematic structure of *LOLA*

Table II
GEAR SIZES, REDUCTION RATIOS AND JOINT WORKING RANGES

Joint[a]		Gear		Torque	Speed	Workspace
		Type[b]	Ratio N	[Nm]	[rad/s]	[deg]
Hip	R	HD	100	284	8.16	± 25
	P	HD	50	370	12.06	$-110 \sim 45$
	Y	HD	100	284	8.16	$-50 \sim 22.5$
Knee	P	RS	≤ 55	390	12.04	$-5 \sim 125$
Ankle	R	RS	≤ 80	286	9.03	± 35
	P	RS	≤ 80	286	9.03	$-62 \sim 45$
Toe	P	HD	100	54	10.68	$-65 \sim 5$
Pelvis	R	HD	100	147	8.16	± 15
	Y	HD	100	147	8.16	± 30
Shoulder	P	HD	100	147	8.16	$-180 \sim 45$
	R	HD	100	110	9.17	$-180 \sim 5$
Elbow	P	HD	100	110	9.17	$-150 \sim 5$

[a]R=roll, P=pitch, Y=yaw. [b]HD=Harmonic Drive, RS=Roller screw.

pelvis has 2 DoFs and each arm has 3 DoFs. A 3-DoF stereo camera head with pan and tilt axes and adjustable camera convergence angle is currently under development.

Considering the leg and pelvis joints, the kinematic chain of the upper body with respect to the stance foot has a redundant structure of 9 DoFs. Kinematic redundancies augment the robot's agility, but they also contribute to reducing the joint loadings: an algorithm is used for redundancy resolution, which minimizes the norm of joint velocities and takes other criteria, such as singularity avoidance and joint limits, into account.

Heel lift-off during terminal stance, which occurs shortly before the swing leg contacts ground, is another measure to reduce the joint loadings. As figured out by KERRIGAN ET AL. [11], heel rise in human gait contributes a considerable portion of the reduction in center of mass (CoM) vertical displacement.

Due to the importance of stance leg heel rise in human walking, the idea of implementing toe joints on a humanoid robot is not new, yet there are only very few humanoid robots with actively driven toe joints, e. g. *H6* and *H7* [12], and the *TOYOTA PARTNER ROBOT* [5]. Recently, OGURA ET AL. [6] presented the robot *WABIAN-2* walking with passive toe joints.

On the other hand, a biped robot with one-piece foot segments is able to perform heel-off only during double support phase, which is implemented in the gait patterns of *JOHNNIE* [13]. During single support, however, the robot would be marginally stable due to the line contact between the foot's leading edge and the floor.

LOLA therefore has an additional, actively driven link between forefoot and heel, which allows the swing leg to be in a more extended configuration. Area contact of the toe segment stabilizes the robot and facilitates forward roll across the forefoot.

B. Overview of Stabilizing Control

Further increasing walking speed, stability and autonomy also requires significant advances in trajectory generation and control algorithms. More accurate models must be used, since effects due to nonlinearities increase at higher walking speeds. Furthermore, the time horizon for trajectory generation must be extended to include not only the current, but also the following steps [14]. *JOHNNIE* is stabilized by modifying the Cartesian coordinates for the following time step. In order to significantly increase walking speed, an additional level of hierarchy will be added to the control architecture of *LOLA*. This layer stabilizes the robot by modifying gait parameters like step length and width and step frequency in real-time.

III. MECHATRONIC DESIGN APPROACH

Fast locomotion poses a significant challenge for biped robots and requires a deliberate design of the mechatronic system. The robot development follows the procedure described by the guideline VDI 2206 "Design methodology for mechatronic systems" [15]. It is an iterative and open-ended process of design and simulation. The multibody simulation model developed by BUSCHMANN [16] is used to obtain the joint loadings, workspaces and the internal forces and moments. It is based on a comprehensive model of the robot and takes into account rotor dynamics, nonlinear gear friction, and electrical dynamics.

Together with assumptions of static loads, the computed data are the basis for the dimensioning of the actuators and structural components. In an early stage, where the link geometry, mass and inertia parameters of *LOLA* were not available, a stable gait pattern for a walking speed of 5 km/h was obtained from the dynamics simulation of the robot *JOHNNIE* by nonlinear parameter optimization [17]. Starting from here, the mechanical structure is developed. After certain milestones of the design have been completed, new inertia properties of the links and actuators are obtained from the 3D-CAD model of the machine, so that both simulation model and CAD design are iteratively refined.

A. General Requirements on the Robot Hardware

The static as well as the dynamic behaviour of the mechanical construction determines the walking performance of the robot. Since the robot's mass and mass distribution have a strong influence on global system dynamics, lightweight construction is of great importance. However, lightness of construction must be balanced with stiffness and the actuator

performance in order to achieve the desired torques and speeds at the required bandwidth.

B. Particular Requirements for High-speed Walking

Besides a suitable kinematic structure, further design goals can be defined to improve the robot hardware for fast walking:

1) high center of mass,
2) low moments of inertia of the leg links.

Unlike humans, the largest portion of a biped robot's weight resides in its legs, since motors and gears determine approximately a third of the overall weight. The center of mass (CoM) height is therefore lower than in humans, typically at the height of the hip joint or even below. According to the *Linear Inverted Pendulum Model* (3D-LIPM) by KAJITA ET AL. [18], the CoM trajectory of the robot is a piecewise hyperbolic curve:

$$y_{\mathrm{CoM}} \sim \cosh\left(\sqrt{\frac{g}{z_{\mathrm{CoM}}}}\, T_s\right)$$

According to this mathematical model, the CoM lateral swing y_{CoM} decreases with higher CoM positions z_{CoM} for a given single support period T_s. Especially at higher walking speeds, the stability of the robot is increased if y_{CoM} is low, because of the reduced angular momentum around the longitudinal axis. Shifting the total CoM as close as possible to the hip joint is therefore a basic design requirement.

But mass distribution in the leg segments is a design variable, which not only affects CoM position, rather, the influence on the inertia of the individual leg segments is much more significant. Therefore, a deliberate design of the leg apparatus is a distinguished means to

- the dynamic performance of the system in general,
- the accuracy of model simplifications, and
- the performance of stabilizing control.

During the final iteration of the mechanical hardware we chose three additional measures to alter mass distribution towards an improved leg dynamics: First, we designed the leg segments as investment castings using topology optimization to balance the conflicting goals of minimal link mass and high stiffness (Section IV-A). Moreover, the mass distribution can strongly be influenced by choosing an appropriate kinematic structure for the leg joint: for the knee joint, a roller screw-based linear actuator is used (Section IV-C); the ankle joint is actuated by a parallel mechanism, where the motors are mounted on the thigh next to the hip joint (Section IV-D).

IV. MECHANICAL DESIGN

A. Design of Structural Components

A detailed analysis by GIENGER [19] shows that the structural components make 43 % of a biped robot's weight. Therefore, the weight of the mechanical structure has to be kept at a minimum, on the other hand, it should show high strength and stiffness to prevent distortion. This is achieved by analyzing all highly loaded components with the finite element method (FEM), where the internal forces and moments are obtained from the multibody simulation model of the robot (see Section III).

Figure 3. Structural components of the pelvis (up) and leg segments (below), manufactured from aluminum by investment casting

Most parts can be designed for low weight and ideal flux of force by intuition and experience. However, if a component has a complex multi-axial stress condition and strict geometric constraints, a solution that satisfies all requirements is difficult to find. Here the topology optimization method has its strengths and aids the development of optimal part geometries. This FEM-based method generates optimal design proposals from supplied packaging information and meets weight or stiffness targets and other constraint criteria such as maximum allowable deflection, stress and method of manufacture. We used *OptiStruct* from *Altair Engineering* to create design proposals for the pelvis, thigh and shank segments. They were designed as investment cast parts made from aluminum (Fig. 3). By using Rapid Prototyping-based manufacturing, there are almost no limitations to a component's shape and it is possible to realize complex, thin-walled part geometries. Several functions could be integrated into a single component part, which led to a reduced part count, and bolted flange connections.

B. Actuator Design

With approximately 31 % the drivetrains make the second largest part of the total weight [19], hence, the development of compact and lightweight joint drives is crucial. We are using high performance permanent magnet synchronous motors (PMSM) from Parker Bayside because of their superior torque and speed capabilities, Fig. 4(a). The motors come as kit motors, which facilitates a space- and weight-saving integration into the joint. Due to the superior characteristics of PMSM, the actuator performance can either be increased without an additional weight gain, or the actuator mass can be decreased in cases where performance enhancement is not needed.

Except for the knee and ankle, all joints employ Harmonic Drive gears as speed reducers, which are the de-facto standard

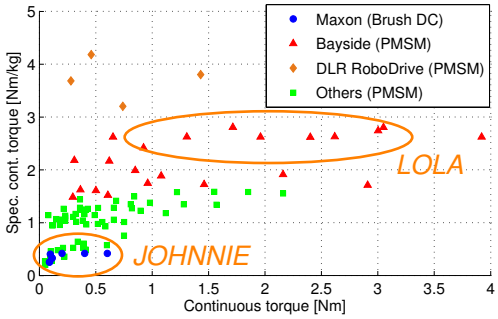

(a) Comparison of the power density of commercially available DC motors and PMSM.

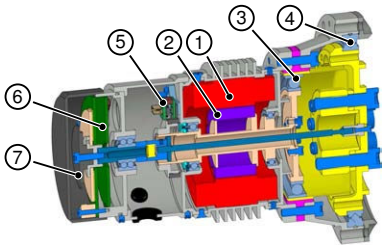

1	Stator winding	5	Incremental encoder
2	Motor shaft	6	Absolute angular sensor
3	Harmonic Drive gear	7	Limit switch
4	Cross roller bearing		

(b) Mechanical design of Harmonic Drive based joints (here: Hip joint yaw axis)

Figure 4. Actuator design

for humanoid robots. Their advantages are well known and include no-backlash and high reduction ratios at a low weight. The compact design of Harmonic Drive component sets allows a space-saving integration directly into the joint units. All gears are custom lightweight versions with a T-shaped Circular Spline which is, in our experience, the best tradeoff between weight and loading capacity. The Wave Generators, modified for low weight and inertia, are made from aluminum or steel. As an example, Fig. 4(b) shows the hip joint yaw axis drive.

C. Knee joint

A Harmonic Drive-based actuator located in the knee joint axis, would unacceptably increase the thigh moment of inertia. In turn, a large part of the enhanced hip joint output would be spent on accelerating the heavier thigh.

By employing the roller screw-based linear drive shown in Fig. 5, mass distribution in the hip-thigh area is significantly improved: The motor is located close to the hip joint rotational axis, so the thigh inertia is reduced by 65 %, and the mass of the actuator itself is reduced by more than 10 % without reducing performance. Thus, the driving power of the knee could be enhanced without decreasing the hip joint's performance. The four-bar linkage mechanism has a nonlinear torque-speed characteristic, similar to the human knee: the maximum torque occurs at around 55°, which is advantageous for typical gait patterns of the robot. Conversely, maximum speeds increase

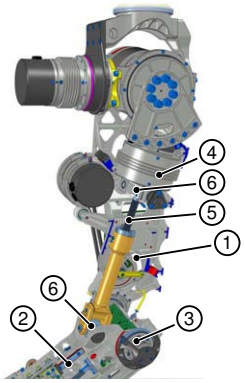

1	Thigh	4	Motor
2	Shank	5	Roller screw
3	Knee joint	6	Universal joint

Figure 5. Knee joint with roller screw-based actuator

at a stretched leg configuration, where they are needed. The linear actuator is backlash-free and back-drivable.

Compared to ballscrews that were used in the first design [20], roller screws have a significantly higher load rating which allowed us to further reduce the drive's weight. Moreover, due to their multi-point contact design, roller screws have the ability to survive shock loads which makes them particularly suitable for the robot's legs.

D. Ankle joint

As shown in [20], the ankle joint axes have clearly different torque-speed characteristics. By employing a parallel drive, the required motor peak torque can be reduced by approx. 35 %. The first design presented in [20] consisted of two coupled four-bar linkage mechanisms, where the motors were directly coupled to the ballscrews. However, since the whole drivetrain was located on the shank segment, this design led to an adverse mass distribution in the legs, the ankle joint workspace was limited, and the ballscrews were not protected from collisions.

The final design is therefore modified towards an improved leg mass distribution and larger workspace. Fig. 6 explains the functionality of the ankle joint actuation: The ankle joint (3) is actuated by two spatial slider-crank mechanisms (7–9), where the motors (4) are mounted on the thigh (1) as close as possible to the hip joint. Each linear drive consists of a roller screw (8) which is mounted on the shank, and a linear bearing (9) to keep the screw free from radial loads. A steering rod (10) connects the linear carriage (7) and the foot segment. The synchronous belt (5) connects the motor shaft (4) to the input shaft of the bevel gear (6) in the knee joint axis. The output shaft of (6) finally drives the roller screw (8), which is arranged in longitudinal direction of the shank and perpendicular to the knee joint axis. The absolute angular sensors (11) allow direct measurement and control of the joint angles.

Even though auxiliary transmissions and couplings were avoided by the first design, these are essential components to achieving a better mass distribution in the legs by spatial separation of electric motor and transmission. The longer

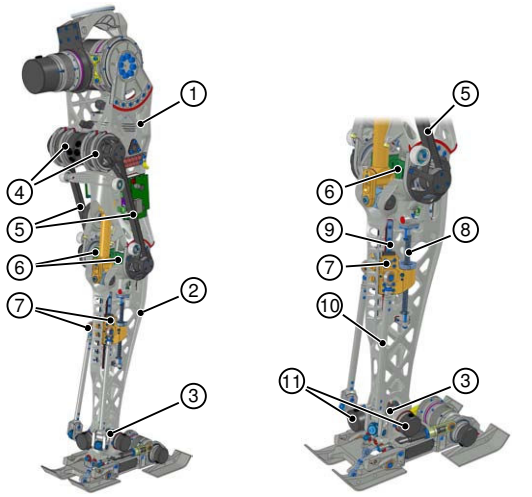

Figure 6. 2-DoF parallel mechanism in the ankle joint of *LOLA*

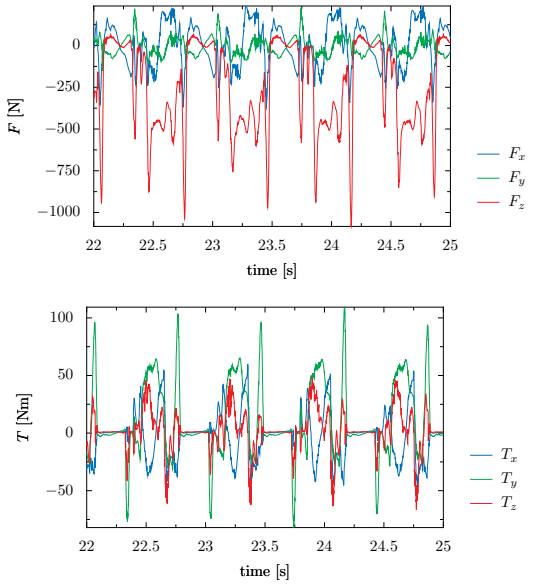

Figure 7. Typical ground reaction forces and moments at a walking speed of 5.5 km/h.

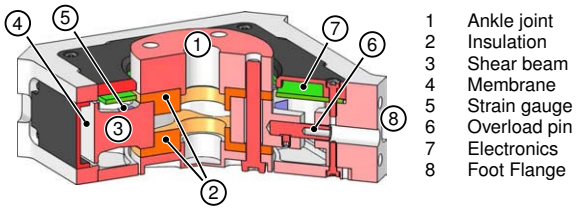

Figure 8. Schematic display of the 6-axis force/torque sensor

transmission distance can reduce inertia and gravity loading, however, it may introduce elasticity and reduce system stiffness. To achieve a high transmission accuracy without adding too much elasticity to the drivetrain, a synchronous belt (6) with a high tensile stregth and an optimized tooth profile is chosen. Moreover, compliance in the belt system is reduced by using a slightly oversized belt, without adding too much weight or inertia to the drivetrain. The bevel gear (6) is a commercial precision gear with minimal backlash ($< 8\,\mathrm{arc\,min}$), which is optimized for position servo applications.

The mechanism is back-drivable and the overall reduction ratio is $N = 80$ at maximum (cf. Table II).

V. Sensor System

A. Joint sensors

Each joint contains several sensors as shown in Fig. 4(b): the incremental rotary encoder (5) mounted on the motor shaft is mainly used for motor control. The absolute angular sensor (6) on the output shaft (resolution 17 bit, accuracy 0.1°) compensates elasticities and nonlinearities in the drivetrain and eliminates the need for a homing routine, enabling the robot to (theoretically) start from arbitrary positions. To improve operational security and to prevent the robot from self-destruction, each joint incorporates a limit switch (7).

B. Inertial measurement unit

The inertial measurement unit (IMU) estimates the orientation and angular velocities of the upper body. From simulations and experiments with *JOHNNIE* we have seen that accuracy and signal quality (i. e. noise) of the IMU significantly determine the performance of the stabilizing controller. Moreover, a low sensor bias results in a low long time drift and a reliable calibration. We are using the IMU *iMAR iVRU-FC-C167* in a custom made lightweight version. It consists of three open-loop fiber-optic gyroscopes and three MEMS accelerometers. The sensor fusion includes internal error models.

C. Force/Torque sensors

LOLA is equipped with two six-axis force/torque sensors that are tightly integrated into the foot structure. Fig. 7 shows the ground reaction forces and moments (walking speed: 5.5 km/h) obtained from the multibody simulation [16].

The sensor (Fig. 8) has a standard Maltese-cross design with four equally spaced and crosswise-arranged shear beams (3). The sensor body has a monolithic structure to avoid hysteresis and setting effects. Each beam holds four strain gauges (5), with two opposing strain gauges connected to half bridges for compensating temperature dependencies. Each shear beam is connected to the sensor body by a thin membrane (4) acting as a flexure hinge which mechanically decouples beam deflection and maximizes strain on the beam surface. To protect the sensor from damage, pin stops (6) engage into the sensor load path and protect the sensing elements at a vertical load corresponding to three times the weight of the robot. As strain gauges are very sensitive to surface leakage currents, the sensor is isolated (2) from the rest of the robot at the ankle joint flange (1).

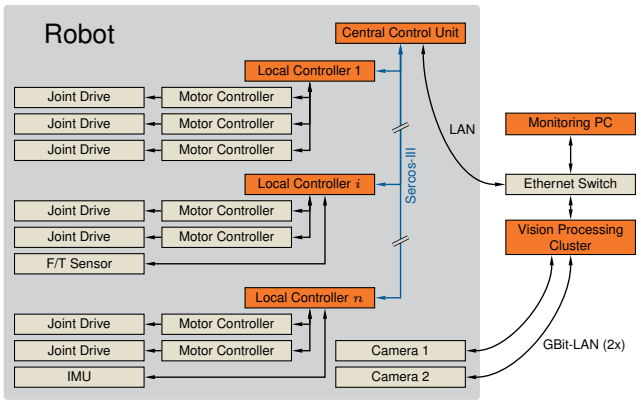

Figure 9. Electronics architecture of *LOLA*

The sensor was calibrated with the least squares method. By applying more than 450 different load cases, a calibration error less than 0.5 % could be achieved. At a total weight of 395 g the sensor includes all necessary electronics and a digital interface.

VI. Electrical/Electronic System

LOLA is controlled by a central control unit mounted on the upper body and several local controllers carrying out low-level tasks, such as link position and velocity control, and sensor data processing. Gait generation and stabilization run on the on-board electronic system without any support from outside except for power supply. An external PC is used only for monitoring purposes and to give basic operating commands if the robot is not connected to the vision system. Due to the high necessary computing power, image data processing is done on an external PC cluster.

Fig. 9 gives a schematic overview of the electronics architecture. The central control unit is based on a PC platform (Core 2 Duo Mobile, 2.33 GHz), running the QNX Realtime Platform. The central control unit and the local controllers are connected via the Ethernet-based real-time communication system Sercos-III. The local controllers are custom-made DSP-based modules, which provide interfaces to the motor controllers and sensors.

VII. Conclusions/Future Work

Despite recent advances, biped walking robots are still slow compared to humans and have limited autonomy. The aim of the research presented here is to diminish this gap. This paper focused on the hardware design of the 25-DoF humanoid robot *LOLA* (180 cm, 55 kg). *LOLA*'s distinctive features are an extremely lightweight construction and a redundant kinematic configuration, which allows for more flexible and natural motions. All joints are equipped with absolute angular sensors and are driven by brushless motors. Special emphasis was put on an improved mass distribution of the leg apparatus to achieve a good dynamic performance. The electronics architecture is designed as an "intelligent" sensor-actuator network with a central controller. The new decentral components increase the system's performance from a technological point of view. *LOLA* will serve as a research platform for fast walking and vision-guided, autonomous locomotion.

Acknowledgement

This work is supported by the "Deutsche Forschungsgemeinschaft" (grant UL 105/29). The authors would like to thank the reviewers for their detailed and helpful comments.

References

[1] M. Hirose and K. Ogawa, "Honda humanoid robots development," *Phil. Trans. R. Soc. A*, vol. 365, pp. 11–19, 2007.
[2] K. Nishiwaki, S. Kagami, J. Kuffner, M. Inaba, and H. Inoue, "Humanoid 'JSK-H7': Research platform for autonomous behavior and whole body motion," in *Proc. Int. Workshop Humanoid and human friendly Robotics (IARP)*, 2002, pp. 2–9.
[3] K. Kaneko, F. Kanehiro, S. Kajita, H. Hirukawa, T. Kawasaki, M. Hirata, K. Akachi, and T. Isozumi, "Humanoid robot HRP-2," in *Proc. IEEE Int. Conf. Rob. Aut. (ICRA)*, 2004, pp. 1083–90.
[4] K. Kaneko, K. Harada, F. Kanehiro, G. Miyamori, and K. Akachi, "Humanoid robot HRP-3," in *Proc. IEEE/RSJ Int. Conf. Rob. Sys. (IROS)*, 2008, pp. 2471–78.
[5] Toyota Motor Corp. (2008) Toyota partner robot. [Online]. Available: http://www.toyota.co.jp/en/tech/robot/p_robot/index.html
[6] Y. Ogura, K. Shimomura, H. Kondo, A. Morishima, T. Okubo, S. Momoki, H. Lim, and A. Takanishi, "Human-like walking with knee stretched, heel-contact and toe-off motion by a humanoid robot," in *Proc. IEEE/RSJ Int. Conf. Rob. Sys. (IROS)*, 2006, pp. 3976–81.
[7] J.-Y. Kim, I.-W. Park, J. Lee, M.-S. Kim, B.-K. Cho, and J.-H. Oh, "System design and dynamic walking of humanoid robot KHR-2," in *Proc. IEEE Int. Conf. Rob. Aut. (ICRA)*, 2005, pp. 1443–48.
[8] K. Löffler, M. Gienger, F. Pfeiffer, and H. Ulbrich, "Sensors and control concept of a biped robot," *IEEE Trans. Ind. Electron.*, vol. 51, no. 5, pp. 972–980, 2004.
[9] S. Kajita, T. Nagasaki, K. Kaneko, K. Yokoi, and K. Tanie, "A hop towards running humanoid biped," in *Proc. IEEE Int. Conf. Rob. Aut. (ICRA)*, 2004, pp. 629–35.
[10] Honda Motor Co., Ltd. (2005, Dec) New ASIMO - running at 6km/h. [Online]. Available: http://world.honda.com/HDTV/ASIMO/New-ASIMO-run-6kmh/
[11] D. Kerrigan, U. Croce, M. M., and P. Riley, "A refined view of the determinants of gait: significance of heel rise," *Arch. Phys. Med. Rehabil.*, vol. 81, pp. 1077–80, 2000.
[12] K. Nishiwaki, S. Kagami, Y. Kuniyoshi, M. Inaba, and H. Inoue, "Toe joints that enhance bipedal and fullbody motion of humanoid robots," in *Proc. IEEE Int. Conf. Rob. Aut. (ICRA)*, 2002, pp. 3105–10.
[13] K. Löffler, *Dynamik und Regelung einer zweibeinigen Laufmaschine*, ser. Fortschrittberichte VDI, Reihe 8. Düsseldorf: VDI-Verlag, 2006, no. 1094.
[14] T. Buschmann, S. Lohmeier, M. Bachmayer, H. Ulbrich, and F. Pfeiffer, "A collocation method for real-time walking pattern generation," in *Proc. Int. Conf. Humanoid Rob. (Humanoids)*, 2007.
[15] *Design methodology for mechatronic systems*, VDI 2206, Jun. 2004.
[16] T. Buschmann, S. Lohmeier, H. Ulbrich, and F. Pfeiffer, "Dynamics simulation for a biped robot: Modeling and experimental verification," in *Proc. IEEE Int. Conf. Rob. Aut. (ICRA)*, 2006, pp. 2673–78.
[17] ——, "Optimization based gait pattern generation for a biped robot," in *Proc. Int. Conf. Humanoid Rob. (Humanoids)*, 2005.
[18] S. Kajita, F. Kanehiro, K. Kaneko, K. Fujiwara, K. Yokoi, and H. Hirukawa, "A realtime pattern generator for biped walking," in *Proc. IEEE Int. Conf. Rob. Aut. (ICRA)*, 2002, pp. 31–7.
[19] M. Gienger, *Entwurf und Realisierung einer zweibeinigen Laufmaschine*, ser. Fortschrittberichte VDI, Reihe 1. Düsseldorf: VDI-Verlag, 2005, no. 378.
[20] S. Lohmeier, T. Buschmann, M. Schwienbacher, H. Ulbrich, and F. Pfeiffer, "Leg design for a humanoid walking robot," in *Proc. Int. Conf. Humanoid Rob. (Humanoids)*, 2006.